EUROPEAN ORGANIZATION FOR NUCLEAR RESEARCH

arXiv:hep-ex/0009017v1 7 Sep 2000

A Study of One-Prong Tau Decays with a Charged Kaon

The OPAL Collaboration

Abstract

From an analysis of the ionisation energy loss of charged particles selected from 110326 $e^+e^- \rightarrow \tau^+\tau^-$ candidates recorded by the OPAL detector at e^+e^- centre-of-mass energies near the Z^0 resonance, we determine the one-prong tau decay branching ratios:

$$\mathrm{Br}(\tau^- \rightarrow \nu_\tau\, K^- \geq 0h^0) = 1.528 \pm 0.039 \pm 0.040\%$$

$$\mathrm{Br}(\tau^- \rightarrow \nu_\tau\, K^-) = 0.658 \pm 0.024 \pm 0.029\%$$

where the h^0 notation refers to a π^0, an η, a K_S^0, or a K_L^0, and where the first uncertainty is statistical and the second is systematic.

(Submitted to European Physics Journal **C**)

The OPAL Collaboration

G. Abbiendi[2], K. Ackerstaff[8], C. Ainsley[5], P.F. Akesson[3], G. Alexander[22], J. Allison[16],
K.J. Anderson[9], S. Arcelli[17], S. Asai[23], S.F. Ashby[1], D. Axen[27], G. Azuelos[18,a],
I. Bailey[26], A.H. Ball[8], E. Barberio[8], R.J. Barlow[16], S. Baumann[3], T. Behnke[25],
K.W. Bell[20], G. Bella[22], A. Bellerive[9], S. Bentvelsen[8], S. Bethke[14,i], O. Biebel[14,i],
I.J. Bloodworth[1], P. Bock[11], J. Böhme[14,h], O. Boeriu[10], D. Bonacorsi[2], M. Boutemeur[31],
S. Braibant[8], P. Bright-Thomas[1], L. Brigliadori[2], R.M. Brown[20], H.J. Burckhart[8],
J. Cammin[3], P. Capiluppi[2], R.K. Carnegie[6], A.A. Carter[13], J.R. Carter[5], C.Y. Chang[17],
D.G. Charlton[1,b], C. Ciocca[2], P.E.L. Clarke[15], E. Clay[15], I. Cohen[22], O.C. Cooke[8],
J. Couchman[15], C. Couyoumtzelis[13], R.L. Coxe[9], M. Cuffiani[2], S. Dado[21],
G.M. Dallavalle[2], S. Dallison[16], A. de Roeck[8], P. Dervan[15], K. Desch[25], B. Dienes[30,h],
M.S. Dixit[7], M. Donkers[6], J. Dubbert[31], E. Duchovni[24], G. Duckeck[31], I.P. Duerdoth[16],
P.G. Estabrooks[6], E. Etzion[22], F. Fabbri[2], M. Fanti[2], L. Feld[10], P. Ferrari[12], F. Fiedler[8],
I. Fleck[10], M. Ford[5], A. Frey[8], A. Fürtjes[8], D.I. Futyan[16], P. Gagnon[12], J.W. Gary[4],
G. Gaycken[25], C. Geich-Gimbel[3], G. Giacomelli[2], P. Giacomelli[8], D. Glenzinski[9],
J. Goldberg[21], C. Grandi[2], K. Graham[26], E. Gross[24], J. Grunhaus[22], M. Gruwé[25],
P.O. Günther[3], C. Hajdu[29], G.G. Hanson[12], M. Hansroul[8], M. Hapke[13], K. Harder[25],
A. Harel[21], C.K. Hargrove[7], M. Harin-Dirac[4], A. Hauke[3], M. Hauschild[8],
C.M. Hawkes[1], R. Hawkings[25], R.J. Hemingway[6], C. Hensel[25], G. Herten[10],
R.D. Heuer[25], M.D. Hildreth[8], J.C. Hill[5], A. Hocker[9], K. Hoffman[8], R.J. Homer[1],
A.K. Honma[8], D. Horváth[29,c], K.R. Hossain[28], R. Howard[27], P. Hüntemeyer[25],
P. Igo-Kemenes[11], K. Ishii[23], F.R. Jacob[20], A. Jawahery[17], H. Jeremie[18], C.R. Jones[5],
P. Jovanovic[1], T.R. Junk[6], N. Kanaya[23], J. Kanzaki[23], G. Karapetian[18], D. Karlen[6],
V. Kartvelishvili[16], K. Kawagoe[23], T. Kawamoto[23], R.K. Keeler[26], R.G. Kellogg[17],
B.W. Kennedy[20], D.H. Kim[19], K. Klein[11], A. Klier[24], T. Kobayashi[23], M. Kobel[3],
T.P. Kokott[3], S. Komamiya[23], R.V. Kowalewski[26], T. Kress[4], P. Krieger[6], J. von
Krogh[11], T. Kuhl[3], M. Kupper[24], P. Kyberd[13], G.D. Lafferty[16], H. Landsman[21],
D. Lanske[14], I. Lawson[26], J.G. Layter[4], A. Leins[31], D. Lellouch[24], J. Letts[12],
L. Levinson[24], R. Liebisch[11], J. Lillich[10], B. List[8], C. Littlewood[5], A.W. Lloyd[1],
S.L. Lloyd[13], F.K. Loebinger[16], G.D. Long[26], M.J. Losty[7], J. Lu[27], J. Ludwig[10],
A. Macchiolo[18], A. Macpherson[28], W. Mader[3], M. Mannelli[8], S. Marcellini[2],
T.E. Marchant[16], A.J. Martin[13], J.P. Martin[18], G. Martinez[17], T. Mashimo[23],
P. Mättig[24], W.J. McDonald[28], J. McKenna[27], T.J. McMahon[1], R.A. McPherson[26],
F. Meijers[8], P. Mendez-Lorenzo[31], F.S. Merritt[9], H. Mes[7], A. Michelini[2], S. Mihara[23],
G. Mikenberg[24], D.J. Miller[15], W. Mohr[10], A. Montanari[2], T. Mori[23], K. Nagai[8],
I. Nakamura[23], H.A. Neal[12,f], R. Nisius[8], S.W. O'Neale[1], F.G. Oakham[7], F. Odorici[2],
H.O. Ogren[12], A. Oh[8], A. Okpara[11], M.J. Oreglia[9], S. Orito[23], G. Pásztor[8,j],
J.R. Pater[16], G.N. Patrick[20], J. Patt[10], P. Pfeifenschneider[14], J.E. Pilcher[9], J. Pinfold[28],
D.E. Plane[8], B. Poli[2], J. Polok[8], O. Pooth[8], M. Przybycień[8,d], A. Quadt[8], C. Rembser[8],
H. Rick[4], S.A. Robins[21], N. Rodning[28], J.M. Roney[26], S. Rosati[3], K. Roscoe[16],
A.M. Rossi[2], Y. Rozen[21], K. Runge[10], O. Runolfsson[8], D.R. Rust[12], K. Sachs[6],

T. Saeki[23], O. Sahr[31], E.K.G. Sarkisyan[22], C. Sbarra[26], A.D. Schaile[31], O. Schaile[31], P. Scharff-Hansen[8], S. Schmitt[11], M. Schröder[8], M. Schumacher[25], C. Schwick[8], W.G. Scott[20], R. Seuster[14,h], T.G. Shears[8], B.C. Shen[4], C.H. Shepherd-Themistocleous[5], P. Sherwood[15], G.P. Siroli[2], A. Skuja[17], A.M. Smith[8], G.A. Snow[17], R. Sobie[26], S. Söldner-Rembold[10,e], S. Spagnolo[20], M. Sproston[20], A. Stahl[3], K. Stephens[16], K. Stoll[10], D. Strom[19], R. Ströhmer[31], B. Surrow[8], S.D. Talbot[1], S. Tarem[21], R.J. Taylor[15], R. Teuscher[9], M. Thiergen[10], J. Thomas[15], M.A. Thomson[8], E. Torrence[9], S. Towers[6], T. Trefzger[31], I. Trigger[8], Z. Trócsányi[30,g], E. Tsur[22], M.F. Turner-Watson[1], I. Ueda[23], P. Vannerem[10], M. Verzocchi[8], H. Voss[8], J. Vossebeld[8], D. Waller[6], C.P. Ward[5], D.R. Ward[5], P.M. Watkins[1], A.T. Watson[1], N.K. Watson[1], P.S. Wells[8], T. Wengler[8], N. Wermes[3], D. Wetterling[11] J.S. White[6], G.W. Wilson[16], J.A. Wilson[1], T.R. Wyatt[16], S. Yamashita[23], V. Zacek[18], D. Zer-Zion[8]

[1]School of Physics and Astronomy, University of Birmingham, Birmingham B15 2TT, UK
[2]Dipartimento di Fisica dell' Università di Bologna and INFN, I-40126 Bologna, Italy
[3]Physikalisches Institut, Universität Bonn, D-53115 Bonn, Germany
[4]Department of Physics, University of California, Riverside CA 92521, USA
[5]Cavendish Laboratory, Cambridge CB3 0HE, UK
[6]Ottawa-Carleton Institute for Physics, Department of Physics, Carleton University, Ottawa, Ontario K1S 5B6, Canada
[7]Centre for Research in Particle Physics, Carleton University, Ottawa, Ontario K1S 5B6, Canada
[8]CERN, European Organisation for Nuclear Research, CH-1211 Geneva 23, Switzerland
[9]Enrico Fermi Institute and Department of Physics, University of Chicago, Chicago IL 60637, USA
[10]Fakultät für Physik, Albert Ludwigs Universität, D-79104 Freiburg, Germany
[11]Physikalisches Institut, Universität Heidelberg, D-69120 Heidelberg, Germany
[12]Indiana University, Department of Physics, Swain Hall West 117, Bloomington IN 47405, USA
[13]Queen Mary and Westfield College, University of London, London E1 4NS, UK
[14]Technische Hochschule Aachen, III Physikalisches Institut, Sommerfeldstrasse 26-28, D-52056 Aachen, Germany
[15]University College London, London WC1E 6BT, UK
[16]Department of Physics, Schuster Laboratory, The University, Manchester M13 9PL, UK
[17]Department of Physics, University of Maryland, College Park, MD 20742, USA
[18]Laboratoire de Physique Nucléaire, Université de Montréal, Montréal, Quebec H3C 3J7, Canada
[19]University of Oregon, Department of Physics, Eugene OR 97403, USA

[20]CLRC Rutherford Appleton Laboratory, Chilton, Didcot, Oxfordshire OX11 0QX, UK
[21]Department of Physics, Technion-Israel Institute of Technology, Haifa 32000, Israel
[22]Department of Physics and Astronomy, Tel Aviv University, Tel Aviv 69978, Israel
[23]International Centre for Elementary Particle Physics and Department of Physics, University of Tokyo, Tokyo 113-0033, and Kobe University, Kobe 657-8501, Japan
[24]Particle Physics Department, Weizmann Institute of Science, Rehovot 76100, Israel
[25]Universität Hamburg/DESY, II Institut für Experimental Physik, Notkestrasse 85, D-22607 Hamburg, Germany
[26]University of Victoria, Department of Physics, P O Box 3055, Victoria BC V8W 3P6, Canada
[27]University of British Columbia, Department of Physics, Vancouver BC V6T 1Z1, Canada
[28]University of Alberta, Department of Physics, Edmonton AB T6G 2J1, Canada
[29]Research Institute for Particle and Nuclear Physics, H-1525 Budapest, P O Box 49, Hungary
[30]Institute of Nuclear Research, H-4001 Debrecen, P O Box 51, Hungary
[31]Ludwigs-Maximilians-Universität München, Sektion Physik, Am Coulombwall 1, D-85748 Garching, Germany

[a] and at TRIUMF, Vancouver, Canada V6T 2A3
[b] and Royal Society University Research Fellow
[c] and Institute of Nuclear Research, Debrecen, Hungary
[d] and University of Mining and Metallurgy, Cracow
[e] and Heisenberg Fellow
[f] now at Yale University, Dept of Physics, New Haven, USA
[g] and Department of Experimental Physics, Lajos Kossuth University, Debrecen, Hungary
[h] and MPI München
[i] now at MPI für Physik, 80805 München
[j] and Research Institute for Particle and Nuclear Physics, Budapest, Hungary.

1   Introduction

Precise studies of the decays of the tau lepton have been made possible by the availability of large, low background tau-pair samples, such as those produced in e^+e^- collisions at CESR and at LEP I. This paper reports on an analysis of one-prong tau decay modes containing a charged kaon, using the complete set of data collected by the OPAL experiment between 1990 and 1995 at e^+e^- centre-of-mass energies near the Z^0 resonance. The excellent charged particle identification capability of the OPAL detector

is exploited to obtain precise measurements of the $\tau^- \to \nu_\tau K^-$ and $\tau^- \to \nu_\tau K^- \geq 0h^0$ branching ratios, where the charge conjugate decays are implied in these interactions and throughout this paper. The h^0 notation refers to a π^0, an η, or a K^0, where the K^0 can be either a K_S^0 or a K_L^0.

Measurements of the $\tau^- \to \nu_\tau K^-$ branching fraction may be used to determine the charged kaon decay constant, f_K, and the CKM matrix element, $|V_{us}|$. In addition, precise measurements of this branching ratio may also be used to set limits on physics beyond the Standard Model, such as charged Higgs effects in tau decays [1].

2   The OPAL Detector

The OPAL detector is described in detail in reference [2]. The component of the detector most important to this analysis is a large volume jet chamber, which measures the momentum and specific ionisation energy loss, dE/dx, of charged particles. The jet chamber provides the only means of distinguishing between charged pions and kaons in the momentum range of interest to this study.

The jet chamber is a cylinder 4 m long and 3.7 m in diameter, and is divided by cathode wire planes into 24 azimuthal sectors. Each sector contains one radial plane of anode wires, which are staggered to resolve left-right ambiguities. The chamber is contained in a solenoidal magnetic field of 0.435 T, and is filled with an argon-methane-isobutane gas mixture at a pressure of 4 atmospheres. This arrangement provides an intrinsic transverse spatial hit resolution of $\sigma_{xy} = 130$ μm, and a two-hit resolution of 2.5 mm.[1] In the barrel region of the jet chamber ($|\cos\theta| < 0.68$), the ionisation energy loss of a charged particle is sampled up to 159 times. A truncated mean is formed by discarding the highest 30% of the measurements, resulting in a dE/dx resolution of 3.1% for isolated tracks in the chamber [3].

Other tracking detectors include a high precision silicon microvertex detector surrounding the beam pipe, a precision gas vertex detector, and a layer of wire chambers with drift direction parallel to the z-axis lying immediately outside the jet chamber. These z-chambers extend to $|\cos\theta| = 0.80$, which encompasses the acceptance of this analysis, and accurately determine the polar angle of charged particles traversing the central detector. A lead-glass electromagnetic calorimeter and presampler chambers are located outside the magnetic coil and jet chamber pressure vessel. The electromagnetic calorimeter is primarily used in this analysis to identify tau decays that include a π^0 or a K^0 in the final state. The return yoke of the OPAL magnet is instrumented

---

[1]A spherical coordinate system is used, with the $+z$-axis in the direction of the circulating electron beam. The angle θ is defined as the polar angle with respect to the $+z$-axis, and ϕ is defined as the azimuthal angle measured from the $+x$-axis, which points towards the centre of the LEP ring.

4

for hadron calorimetery, and is surrounded by external muon chambers. The hadron calorimeter and muon chambers are mainly used in this analysis to select control samples containing muons and to veto non-tau backgrounds in the tau-pair candidate sample.

2.1 Parameterisation of Ionisation Energy Loss

The mean ionisation energy lost per unit distance by a particle of charge q and speed β traversing a gas is approximately described by the Bethe-Bloch equation [4, 5]:

$$D_{\mathrm{pred}} = -\frac{A_1 q^2}{\beta^2} \left[A_2 + \ln\left(\gamma^2 \beta^2\right) - \beta^2 - \delta(\beta)/2 \right], \qquad (1)$$

where A_1 and A_2 are constants which depend on the gas composition, and $\delta(\beta)$ is a function which describes polarisation effects in the gas.

The ionisation energy loss parameterisation used by OPAL, D_{pred}, is a variation of the Sternheimer-Peierls modification to the Bethe-Bloch formula [3, 6], and uses six input parameters. Figure 1(a) shows the dependence of $\mathrm{d}E/\mathrm{d}x$ on the momentum of various particles in the OPAL jet chamber, as predicted by D_{pred}. Figure 1(b) shows the particle resolving power, $\mathcal{R}_{ij}$, versus momentum for various pairs of particle species i and j, where:

$$\mathcal{R}_{ij} \equiv |D^i_{\mathrm{pred}} - D^j_{\mathrm{pred}}| \, / \, \sigma,$$

and where σ is the resolution of the measured $\mathrm{d}E/\mathrm{d}x$. Note that the OPAL jet chamber yields a pion/kaon separation of at least 2σ for particles between about 2 to 30 GeV/c.

The parameters used in the calculation of D_{pred} and σ are tuned to the measured energy loss of charged particles in hadronic $\mathrm{Z}^0 \to q\bar{q}$ decays, yielding a $\mathrm{d}E/\mathrm{d}x$ parameterisation that is accurate enough for nearly all analyses of OPAL data.

However, hadronic $\mathrm{Z}^0 \to q\bar{q}$ decays tend to have a much higher track multiplicity than one-prong tau decays, leading to small systematic differences between the measured $\mathrm{d}E/\mathrm{d}x$ in the two environments. Although these differences are less than one σ in magnitude, they must be corrected for accurate particle identification in one-prong tau decays. Based on a study of the measured energy loss of muons in $\mathrm{e}^+\mathrm{e}^- \to \mu^+\mu^-$, $\tau^- \to \mu^- \overline{\nu}_\mu \nu_\tau$, and $\mathrm{e}^+\mathrm{e}^- \to \mathrm{e}^+\mathrm{e}^- \mu^+\mu^-$ control samples, the following corrections are applied to the the OPAL $\mathrm{d}E/\mathrm{d}x$ parameterisation, D_{pred}, and to the measured energy loss and its uncertainty, D_{meas} and σ:

Multiplicative correction to D_{pred} : To obtain a parameterisation which correctly predicts the measured energy loss of particles from tau decays, D_{pred} must be corrected with a multiplicative factor, $s(\beta)$. Parameterising $s(\beta)$ as a second order

polynomial in $-\log(1 - \beta^2)$ yields satisfactory results. The magnitude of the correction is of order 1% for tracks in one-prong tau decays.

Additive correction to D_{meas} : The measured energy loss of charged particles in low-multiplicity events is found to depend strongly on the azimuthal separation, ϕ, between the track and anode plane in the jet chamber cell. To improve the dE/dx resolution, this behaviour is corrected with a function, $f(\phi)$, with seven parameters tuned to the measured energy loss of $e^+e^- \to \mu^+\mu^-$ candidates. The magnitude of this correction is also of order 1%.

Multiplicative correction to σ: To correctly predict the spread in the dE/dx of charged particles from one-prong tau decays, the OPAL parameterisation of σ must be corrected with a multiplicative factor, $s_{\mathrm{res}} \approx 0.9$.

3   Monte Carlo Generated Event Samples

For this analysis, tau lepton decays are simulated with the KORALZ 4.0 Monte Carlo generator and the TAUOLA 2.4 decay package [7, 8]. A Monte Carlo sample of 600000 tau-pair events is generated with input branching ratios determined from world averages or theoretical expectations [9]. Background contributions from non-τ sources were evaluated using Monte Carlo samples obtained from the following generators: hadronic $Z^0 \to q\bar{q}$ events were simulated using JETSET 7.4 [10], $e^+e^- \to \mu^+\mu^-$ events using KORALZ, Bhabha events using BABAMC [11] and BHWIDE [12], and four-fermion events using VERMASEREN 1.01 [13] and FERMISV [14].

All Monte Carlo samples are passed through a detailed simulation of the OPAL detector [15] and are subjected to the same analysis chain as the data.

4   Data Selection

This analysis uses the full data set collected by the OPAL detector in the years 1990 through 1995 at e^+e^- centre-of-mass energies close to the Z^0 resonance. Only data for which the tracking chambers and the electromagnetic calorimeter were fully operational are retained. The topology of $e^+e^- \to \tau^+\tau^-$ events is characterised by a pair of back-to-back, narrow jets with low particle multiplicity. Jets are defined in this analysis by grouping tracks and electromagnetic clusters into cones with a half-angle of $35°$, where each cone is assumed to contain the decay products of one of the tau leptons. Tau-pair candidates are selected by requiring two low-multiplicity jets ($N_{\mathrm{track}} \leq 6$) with an average polar angle of $|\cos\theta_{\mathrm{ave}}| < 0.68$. Background events from other lepton pairs,

hadronic $Z^0 \to q\bar{q}$ decays, and four-fermion events are reduced with cuts on the event topology and total visible energy. These selections produce a sample of 110326 tau-pair candidates with background $f^{\mathrm{non}-\tau} = 1.56 \pm 0.10\%$, estimated by data control samples and Monte Carlo background samples. The tau-pair selection procedure is described in detail in reference [16].

One-prong tau decays are selected from this sample by choosing tau decay cones containing only one well-reconstructed charged track, consistent with coming from the origin. Tracks in this sample are required to have at least 40 jet chamber hits used in the calculation of the measured $\mathrm{d}E/\mathrm{d}x$, to have at least 3 hits in the $z-$chambers, and to have reconstructed momentum between 2 and 50 GeV/c. A sample of 143528 candidates is selected by this procedure.

The number of charged kaons in the sample is determined by maximising a likelihood function based on $\mathrm{d}E/\mathrm{d}x$. The $\tau^- \to \nu_\tau \, \mathrm{K}^- \geq 0\mathrm{h}^0$ branching ratio is then obtained by correcting the number of kaons for backgrounds and selection inefficiencies. As a cross-check of the general analysis procedure, the $\tau^- \to \nu_\tau \, \pi^- \geq 0\mathrm{h}^0$ branching ratio is also determined in an analogous fashion, and compared to the world average.

5   Inclusive $\tau^- \to \nu_\tau \, \mathrm{K}^- \geq 0\mathrm{h}^0$ Branching Ratio

The tracks in the one-prong tau decay candidate sample consist of electrons, muons, pions, and kaons from both tau decays and non-tau sources. To determine the number of charged kaons in the sample, a maximum likelihood fit to the ionisation energy loss distribution of the tracks in the sample is performed. The likelihood function used in the fit is:

$$\mathcal{L} = \exp\left[-\tfrac{1}{2}\left(\frac{f'_\mu - f_\mu}{\Delta f'_\mu}\right)^2\right] \prod_{j=1,N} \sum_{k=\mathrm{e},\mu,\pi,\mathrm{K}} f_k \, W^{kj}, \tag{2}$$

where W^{kj} is the $\mathrm{d}E/\mathrm{d}x$ weight of charged particle j under particle hypothesis k,

$$W^{kj} = \frac{1}{\sqrt{2\pi}s(\beta_j)s_{\mathrm{res}}\sigma_{kj}} \, \exp\left[-\frac{1}{2}\left(\frac{D^j_{\mathrm{meas}} - f(\phi_j) - s(\beta_j)D^{kj}_{\mathrm{pred}}}{s(\beta_j)s_{\mathrm{res}}\sigma_{kj}}\right)^2\right], \tag{3}$$

and where

f_k is the fraction of particle type k in the sample, where k is either pion, kaon, muon, or electron. The values of f_k are constrained to be non-negative, and their sum is constrained to be 1.

7

f'_μ and $\Delta f'_\mu$ are the fraction, and uncertainty on the fraction, of muons in the sample, as estimated by Monte Carlo generated events. The estimated muon fraction is corrected using information from data and Monte Carlo muon control samples that are selected using information from the OPAL muon chambers. This constraint is added to the fit to help distinguish between pions and muons in the sample, which have quite similar $\mathrm{d}E/\mathrm{d}x$.

N is the total number of particles in the sample.

D^j_{meas} is the measured $\mathrm{d}E/\mathrm{d}x$ of the jth charged particle.

D^{kj}_{pred} is the predicted $\mathrm{d}E/\mathrm{d}x$ for charged particle j, calculated with the OPAL parameterisation under particle hypothesis k, as obtained from the measured $\mathrm{d}E/\mathrm{d}x$ of charged particles in hadronic $\mathrm{Z}^0 \to q\bar{q}$ events.

σ_{kj} is the $\mathrm{d}E/\mathrm{d}x$ uncertainty, calculated using the OPAL parameterisation, as obtained from the measured $\mathrm{d}E/\mathrm{d}x$ of hadronic $\mathrm{Z}^0 \to q\bar{q}$ events.

s_{res} is the multiplicative correction to σ_{kj}, as determined from the one-prong control samples as described in Section 2.1.

$s(\beta)$ is the β dependent multiplicative correction to D_{pred}, as determined from the one-prong control samples.

$f(\phi)$ is the ϕ dependent correction to the measured $\mathrm{d}E/\mathrm{d}x$, as obtained from the one-prong control samples.

Efforts are made to obtain a $\mathrm{d}E/\mathrm{d}x$ parameterisation for the tau decay environment that is optimal for many particle species over a wide range of momenta. However, it is possible that the $\mathrm{d}E/\mathrm{d}x$ corrections described in Section 2.1 may be somewhat more (or less) optimal for pions than they are for kaons in the momentum range of interest. Thus, to correct for any possible species-dependent quality differences in the parameterisation of $\mathrm{d}E/\mathrm{d}x$, an extra factor, C_{K}, is allowed to multiply the kaon predicted energy loss, $D^{\mathrm{K}}_{\mathrm{pred}}$, and is allowed to vary freely in the fit using the likelihood function found in Equation 2. The value of C_{K} returned by the fit is $C_{\mathrm{K}} = 0.9943 \pm 0.0009$.

Independent likelihood fits are performed in 13 momentum bins of variable size in the range of 2 to 50 GeV/c. A test of the fit with Monte Carlo generated samples verifies that the resulting estimates for the kaon fraction are efficient and unbiased.

The number of charged kaons and pions found in the sample, summed over all momentum bins, is given in Table 1, and the stretch $\mathrm{d}E/\mathrm{d}x$ distribution of tracks in all momentum bins of the sample is shown in Figure 2. Stretch energy loss, S_i, is defined as:

$$S_i = (D_{\mathrm{meas}} - D^i_{\mathrm{pred}})/\sigma,$$

where i is the particle hypothesis used to calculate the predicted dE/dx. The normalisation of the predicted distributions of the kaons, pions, muons, and electrons in Figure 2 is obtained from the results of the likelihood fit. The momentum distributions of the charged kaons and pions in the sample, as estimated by the likelihood fit, are shown in Figure 3.

5.1 The Branching Ratio Calculation

To determine the $\tau^- \to \nu_\tau K^- \geq 0h^0$ branching ratio, the number of charged kaons found by the dE/dx likelihood fit in the one-prong candidate sample is corrected for backgrounds and selection inefficiencies:

$$B_{K^- \geq 0h^0} \equiv \mathrm{Br}(\tau^- \to \nu_\tau K^- \geq 0h^0) = \frac{N^K_{\mathrm{TOTAL}} - N^K_{\mathrm{bkgnd}}}{\epsilon_{K^- \geq 0h^0} N_\tau (1 - f^{\mathrm{non}-\tau})}, \tag{4}$$

where

N_τ is the number of tau decay candidates. There were 220652 tau decay candidates recorded in the barrel region of the OPAL detector between the years 1990 and 1995.

$f^{\mathrm{non}-\tau}$ is the estimated background from non-τ sources in the tau decay candidates ($f^{\mathrm{non}-\tau} = 1.56 \pm 0.10\%$).

N^K_{TOTAL} is the total number of kaons in the one-prong tau decay sample, as estimated by the likelihood fit. The number of kaons summed over all momentum bins in the sample is shown in Table 1.

N^K_{bkgnd} is the number of background kaons in the one-prong tau decay sample, as estimated by Monte Carlo generated tau decay and hadronic $Z^0 \to q\bar{q}$ samples. The number of background kaons summed over all momentum bins in the sample is shown in Table 1.

$\epsilon_{K^- \geq 0h^0}$ is the efficiency for $\tau^- \to \nu_\tau K^- \geq 0h^0$ decays in the tau-pair candidate sample to contribute kaons to the one-prong tau decay sample, and is shown in Table 1. The efficiency has been corrected for biases introduced by the tau-pair selection procedure, and the uncertainty on the efficiency includes the systematic uncertainty arising from this correction. The bias corrections are all consistent with 1 to within one standard deviation of their Monte Carlo statistical uncertainties.

The result of the branching ratio calculation is:

$$B_{K^- \geq 0h^0} = 1.528 \pm 0.039 \pm 0.040\%,$$

where the first uncertainty is statistical and the second is systematic. A summary of the systematic uncertainties, all of which will be described in subsequent sections, is shown in Table 3.

As a cross-check of the general analysis procedure, we also determine the $\tau^- \to \nu_\tau \pi^- \geq 0h^0$ branching ratio. Thus, in a similar manner to the $\tau^- \to \nu_\tau K^- \geq 0h^0$ branching ratio calculation, the total number of charged pions found in the one-prong tau decay sample by the likelihood fit is corrected for backgrounds and the $\tau^- \to \nu_\tau \pi^- \geq 0h^0$ efficiency to yield $B_{\pi^- \geq 0h^0} = 48.26 \pm 0.25\%$, where the uncertainty is statistical only. The linear correlation coefficient between the OPAL $\tau^- \to \nu_\tau K^- \geq 0h^0$ and $\tau^- \to \nu_\tau \pi^- \geq 0h^0$ branching ratios is approximately -20%. The OPAL $\tau^- \to \nu_\tau \pi^- \geq 0h^0$ branching ratio is consistent with the world average, derived from the branching ratios of the tau to the various exclusive final states that include a charged pion listed in reference [17], $B_{\pi^- \geq 0h^0} = 48.36 \pm 0.23\%$, and thus we conclude that biases introduced by the analysis procedure are negligible.

5.2 dE/dx Systematic Studies

A significant source of systematic uncertainty in the measurement of the inclusive branching ratio is the uncertainty in the parameterisation of the predicted energy loss. To assess this systematic, we determine the sensitivity of the likelihood estimates of the number of kaons within the data sample to the uncertainties in the dE/dx correction factors obtained from the one-prong control samples. The likelihood function shown in Equation 2 is therefore modified such that:

$$\mathcal{L}' = \exp\left(-\tfrac{1}{2}\left(\mathbf{n}' - \mathbf{n}\right)^{\mathbf{T}}\mathbf{V}^{-1}(\mathbf{n}' - \mathbf{n})\right)\mathcal{L},$$

where

$\mathbf{n}'$ is a vector containing the central values of the dE/dx correction factors that describe the functions $f(\phi)$, $s(\beta)$, and s_{res}, where the central values are as obtained from the fits to the one-prong control samples.

$\mathbf{n}$ is a vector containing the dE/dx correction factors used in the likelihood fit.

$\mathbf{V}$ is the covariance matrix for the dE/dx correction factors, as obtained from the fits to the one-prong control samples.

A 'prior-belief' method is used to assess the systematic uncertainty; in the first iteration of the fit, the correction factors are allowed to vary, and the returned values are found to be consistent with the values obtained from the control samples. In the second iteration, the likelihood fit is repeated, this time keeping the dE/dx correction

10

factors fixed to the values from the first iteration. The systematic uncertainty in $N^{\mathrm{K}}_{\mathrm{TOTAL}}$ (and N^{π}_{TOTAL}) due to the parameterisation of $\mathrm{d}E/\mathrm{d}x$ is then obtained from the square root of the quadrature difference of the fit uncertainties in $N^{\mathrm{K}}_{\mathrm{TOTAL}}$ (N^{π}_{TOTAL}) from the two iterations, and is shown in Table 1.

5.3   Efficiency Estimation

The efficiencies for kaons and pions from signal events in the tau-pair candidate sample to enter the data sample are estimated using signal events generated with the KORALZ 4.0 Monte Carlo generator and the TAUOLA 2.4 decay package, as described in Section 3. The efficiency for $\tau^- \to \nu_\tau \, \mathrm{K}^- \geq 0\mathrm{h}^0$ decays in the tau-pair candidate sample to contribute to the one-prong sample, $\epsilon_{\mathrm{K}^- \geq 0\mathrm{h}^0}$, is calculated via:

$$\epsilon_{\mathrm{K}^- \geq 0\mathrm{h}^0} = f \epsilon_{\mathrm{K}^-} + (1 - f) \epsilon_{\mathrm{K}^- \geq 1\mathrm{h}^0},$$

where f is the ratio of the exclusive $\tau^- \to \nu_\tau \, \mathrm{K}^-$ branching ratio to the inclusive $\tau^- \to \nu_\tau \, \mathrm{K}^- \geq 0\mathrm{h}^0$ branching ratio, as obtained from OPAL data (see Section 6.2). The $\epsilon_{\mathrm{K}^- \geq 1\mathrm{h}^0}$ efficiency is calculated from the average of the relevant efficiencies appearing in Table 2, weighted by the associated world average branching ratios. The inclusive and exclusive branching ratios determined by this analysis are all less than 15% correlated with the world average branching ratios used in this efficiency calculation. All efficiencies have been corrected for biases introduced by the tau-pair selection procedure, and, in addition, the Monte Carlo efficiency estimates for the signal events to pass the jet chamber and z-chamber hit requirements are corrected using a control sample of data one-prong tau decays. The uncertainty on each efficiency includes the systematic uncertainties arising from these corrections.

The efficiency for $\tau^- \to \nu_\tau \, \pi^- \geq 0\mathrm{h}^0$ decays in the tau-pair candidate sample to contribute to the one-prong sample, $\epsilon_{\pi^- \geq 0\mathrm{h}^0}$, is calculated using the same procedure, except that the ratio of the $\tau^- \to \nu_\tau \, \pi^-$ branching ratio relative to the $\tau^- \to \nu_\tau \, \pi^- \geq 0\mathrm{h}^0$ branching ratio is taken from world averages.

The Monte Carlo modelling of the probability for photons to convert to an $\mathrm{e}^+\mathrm{e}^-$ pair in the OPAL detector material has been found by previous studies of data control samples to be correct to within an absolute uncertainty of about $\pm 0.5\%$ [18]. To assess the systematic uncertainty in the branching fraction associated with this modelling, we determine the change in the branching fraction when the efficiency for each exclusive final state is changed by $+0.005$ for each associated photon in the final state; thus the efficiency for $\tau^- \to \nu_\tau \, \mathrm{K}^- \pi^0$ decays is changed by $2 \times 0.005 = 0.01$, and the efficiency for $\tau^- \to \nu_\tau \, \mathrm{K}^- \pi^0 \pi^0$ decays is changed by $4 \times 0.005 = 0.02$. We also determine the change in the branching fraction when the efficiency for each exclusive final state is changed by -0.005 for each associated photon in the final state. The resulting systematic uncertainties in the branching fractions are shown in Table 3.

The variation of the branching ratio due to alternative intermediate resonant structure scenarios for the $\tau^- \to \nu_\tau \, K^- \pi^0 \pi^0$ final state is assessed using efficiency estimates from signal events generated by the modified version of TAUOLA 2.4 through non-resonant production only. The efficiency calculated from this sample for $\tau^- \to \nu_\tau \, K^- \pi^0 \pi^0$ to contribute to the data candidates is within 0.4σ of the central value, where σ represents the combined Monte Carlo statistical uncertainties. Since the two different scenarios produce consistent results for the efficiency, and since there is no *a priori* reason to expect a strong efficiency dependence on the intermediate resonant structure, no systematic uncertainty for this effect is assigned.

In a similar fashion, the variation of the branching ratio due to alternative intermediate resonant structure scenarios for the $\tau^- \to \nu_\tau \, K^- K^0 \pi^0$ final state is explored using events generated through non-resonant production only. The $\tau^- \to \nu_\tau \, K^- K^0 \pi^0$ efficiency calculated from these events is within 0.6σ of the central value, thus no additional systematic uncertainty is assigned.

Since the observed momentum distributions for both the pions and the kaons in the sample are well described by the Monte Carlo generated events, no systematic uncertainty is assigned for possible error in either the estimate of the total efficiency, or the momentum dependence of the efficiency estimates, since it is apparent that such errors are small relative to the other systematic uncertainties, as listed in Table 3.

5.4 Background Estimation

The number of background kaons in $N_{\mathrm{TOTAL}}^{\mathrm{K}}$ is estimated by applying the same selection criteria to Monte Carlo samples of hadronic $Z^0 \to q\bar{q}$ decays and three-prong tau decays. From the number of selected events that contain kaons, the estimated number of background kaons is derived, as summarised in Table 1. There are very few background kaons in $N_{\mathrm{TOTAL}}^{\mathrm{K}}$, most of which result from the small amount of low-multiplicity hadronic $Z^0 \to q\bar{q}$ events contaminating the tau-pair sample. Due to this small contamination, the systematic uncertainty associated with the background correction is neglible.

The number of background pions in N_{TOTAL}^{π} is estimated in a comparable manner.

6   Exclusive Branching Ratios

To distinguish between one-prong tau final states with and without accompanying neutral particles, information from the electromagnetic calorimeter is used. Tau decays that include neutral particles tend to have a larger relative electromagnetic energy

deposition, E/p, associated with the tau decay cone than tau decays without accompanying neutrals. Such decays also tend to have a larger number of associated clusters, N_{clus}, in the electromagnetic calorimeter than tau decays without neutrals. To ensure accurate modelling of the E/p and N_{clus} distributions of one-prong tau decays to charged kaons, corrections to the Monte Carlo simulation are obtained from a data $\tau^- \rightarrow \nu_\tau \pi^- \geq 0h^0$ control sample. The following sections describe these corrections, and how they are applied in the determination of the $\tau^- \rightarrow \nu_\tau K^-$ branching ratio.

6.1 Corrections to the Modelling of E/p and N_{clus}

The two-dimensional $(p, E/p)$ and (p, N_{clus}) distributions of data $\tau^- \rightarrow \nu_\tau \pi^- \geq 0h^0$ decays are used to determine corrections to the Monte Carlo modelling of the E/p and N_{clus} distributions of $\tau^- \rightarrow \nu_\tau K^- \geq 0h^0$ decays. To this end, the data one-prong tau decay sample is divided into 13 bins of momentum between 2 to 50 GeV/c and 6 bins of E/p, and the number of charged pions and kaons within each bin is determined by maximising the dE/dx likelihood function shown in Equation 2. After background correction, this procedure yields the $(p, E/p)$ distributions of $\tau^- \rightarrow \nu_\tau \pi^- \geq 0h^0$ and $\tau^- \rightarrow \nu_\tau K^- \geq 0h^0$ decays. The data one-prong sample is also divided into 13 bins of momentum and 4 bins of N_{clus}, and the (p, N_{clus}) distributions of $\tau^- \rightarrow \nu_\tau \pi^- \geq 0h^0$ and $\tau^- \rightarrow \nu_\tau K^- \geq 0h^0$ decays are determined in a comparable manner.

The momentum distribution of the charged pions in the one-prong tau decay sample, as shown in Figure 3, appears to be adequately modelled by Monte Carlo generated $\tau^- \rightarrow \nu_\tau \pi^- \geq 0h^0$ events. However, the E/p and N_{clus} distributions, obtained by summing the $(p, E/p)$ and (p, N_{clus}) distributions over momentum bins, are not as well modelled by the Monte Carlo, as is shown in Figure 4.

6.1.1 Corrections to E/p

Separate corrections are derived for the Monte Carlo E/p modelling of $\tau^- \rightarrow \nu_\tau \pi^-$, $\tau^- \rightarrow \nu_\tau \pi^- \pi^0$, and $\tau^- \rightarrow \nu_\tau \pi^- \pi^0 \pi^0$ decays. These three decay modes produce 95% of the charged pions found in the one-prong tau decay sample. The E/p corrections obtained for $\tau^- \rightarrow \nu_\tau \pi^-$ are applied to the Monte Carlo modelling of the E/p of $\tau^- \rightarrow \nu_\tau K^-$, and, in a similar fashion, the corrections to the E/p distribution of $\tau^- \rightarrow \nu_\tau \pi^- \pi^0$ $(\tau^- \rightarrow \nu_\tau \pi^- \pi^0 \pi^0)$ decays are applied to that of $\tau^- \rightarrow \nu_\tau K^- h^0$ $(\tau^- \rightarrow \nu_\tau K^- \geq 2h^0)$ decays.

The corrections to the $\tau^- \rightarrow \nu_\tau \pi^-$, $\tau^- \rightarrow \nu_\tau \pi^- \pi^0$, and $\tau^- \rightarrow \nu_\tau \pi^- \pi^0 \pi^0$ Monte Carlo modelling of E/p are obtained by first correcting the number of charged pions within each $(p, E/p)$ bin of the one-prong tau decay sample for background pions from

13

hadronic $Z^0 \rightarrow q\bar{q}$ events. The number of pions in each bin is also corrected for the number of pions from tau sources other than $\tau^- \rightarrow \nu_\tau \pi^-$, $\tau^- \rightarrow \nu_\tau \pi^- \pi^0$, and $\tau^- \rightarrow \nu_\tau \pi^- \pi^0 \pi^0$ decays using world average branching ratios and information from Monte Carlo generated events. The following χ^2 function is then minimised:

$$\chi^2 = \sum_i \sum_j \left[\frac{(N_{ij}^\pi - \sum_l N_\tau (1 - f^{\mathrm{non}-\tau}) \epsilon_l \mathrm{B}_l \, s_i^l \, S_{ij}^l \, \mathcal{S}_j^l)}{\Delta N_{ij}^\pi} \right]^2 , \tag{5}$$

where the index i runs over the momentum bins, the index j runs over the E/p bins, and the index l runs over $\tau^- \rightarrow \nu_\tau \pi^-$, $\tau^- \rightarrow \nu_\tau \pi^- \pi^0$, and $\tau^- \rightarrow \nu_\tau \pi^- \pi^0 \pi^0$. Also:

N_{ij}^π is the number of charged pions, after corrections for non-$\tau^- \rightarrow \nu_\tau \pi^- \leq 2\pi^0$ background, found by the $\mathrm{d}E/\mathrm{d}x$ likelihood fit in the $(i,j)^{\mathrm{th}}$ bin of the $(p, E/p)$ distribution of one-prong tau decays.

ΔN_{ij}^π is the statistical uncertainty on N_{ij}^π, as obtained from the $\mathrm{d}E/\mathrm{d}x$ likelihood fit.

B_l is the world average branching ratio of tau decay l, taken from reference [17].

ϵ_l is the efficiency for events from tau decay l in the tau-pair candidate sample to contribute to the one-prong tau decay sample.

S_{ij}^l is the probability, calculated using Monte Carlo generated events, for tau decays of type l in the one-prong tau decay sample to contribute to the $(i,j)^{\mathrm{th}}$ bin of the $(p, E/p)$ distribution.

$\mathcal{S}_j^l$ is the correction to the jth bin of the Monte Carlo E/p distribution of tau decays of type l. The $\mathcal{S}_j^l$ are the only parameters allowed to float freely in the fit.

s_i^l is a normalisation factor used to ensure that the correction to E/p does not affect the shape of the momentum distribution of decays of type l, and is determined from the condition $\sum_j s_i^l S_{ij}^l \mathcal{S}_j^l = P_i^l$, where P_i^l is the probability, as calculated from Monte Carlo generated events, for tau decays of type l to contribute to the ith bin of the momentum distribution.

6.1.2   Corrections to N_{clus}

Corrections, $\mathcal{T}$, to the Monte Carlo modelling of N_{clus} of $\tau^- \rightarrow \nu_\tau \pi^-$, $\tau^- \rightarrow \nu_\tau \pi^- \pi^0$, and $\tau^- \rightarrow \nu_\tau \pi^- \pi^0 \pi^0$ decays are obtained in a comparable manner to the method used to obtain the E/p corrections. Again, the $\tau^- \rightarrow \nu_\tau \pi^-$, $\tau^- \rightarrow \nu_\tau \pi^- \pi^0$, and $\tau^- \rightarrow \nu_\tau \pi^- \pi^0 \pi^0$ N_{clus} distributions are similar to those of $\tau^- \rightarrow \nu_\tau \mathrm{K}^-$, $\tau^- \rightarrow \nu_\tau \mathrm{K}^- \mathrm{h}^0$, and $\tau^- \rightarrow \nu_\tau \mathrm{K}^- \geq 2\mathrm{h}^0$ decays, respectively.

The absolute linear correlation coefficients between N_{clus} and p, and N_{clus} and E/p are less than 20% in all classes of signal. Thus, the N_{clus} and the $(p, E/p)$ distributions are used as discriminators in this analysis, and N_{clus} is treated as a variable uncorrelated to both p and E/p.

6.2 The $\tau^- \to \nu_\tau \, \mathrm{K}^-$ Branching Ratio

The $\tau^- \to \nu_\tau \, \mathrm{K}^-$ branching ratio, $\mathrm{B}_{\mathrm{K}^-}$, is determined by a χ^2 fit to the $(p, E/P)$ and N_{clus} distributions of one-prong tau decays with a charged kaon, where the modelling of the distributions is corrected using the results of the previous section. The following χ^2 is minimised:

$$
\begin{aligned}
\chi^2 \;=\; & \sum_j \sum_i \left[\frac{N_{ij}^{\mathrm{K}} - N_{ij}^{\text{bkgnd}} - \sum_l \epsilon_l s_i^l S_{ij}^l G_j^l R}{\Delta N_{ij}^{\mathrm{K}}} \right]^2 \\
& + \sum_k \left[\frac{N_k^{\mathrm{K}} - N_k^{\text{bkgnd}} - \sum_l \epsilon_l T_k^l H_k^l R}{\Delta N_k^{\mathrm{K}}} \right]^2 ,
\end{aligned}
\tag{6}
$$

where l is an index referring to either $\tau^- \to \nu_\tau \, \mathrm{K}^-$, $\tau^- \to \nu_\tau \, \mathrm{K}^- \mathrm{h}^0$, or $\tau^- \to \nu_\tau \, \mathrm{K}^- \geq 2\mathrm{h}^0$, and the indices i, j, and k run over the p, E/p, and N_{clus} bins, respectively. The number of background kaons within each bin is N^{bkgnd}, while ΔN^{K} is the statistical uncertainty on the number of kaons within each bin, N^{K}. Also:

$$
\begin{aligned}
R \;&=\; \frac{N_{\text{TOTAL}}^{\mathrm{K}}}{f\epsilon_{\mathrm{K}^-} + (1-f)\epsilon_{\mathrm{K}^- \geq 1\mathrm{h}^0}} \\
G_j^{\mathrm{K}^-} \;&=\; \mathcal{S}_j^{\pi^-} f \\
G_j^{\mathrm{K}^- \mathrm{h}^0} \;&=\; \mathcal{S}_j^{\pi^- \pi^0} (1-f) \frac{\mathrm{B}_{\mathrm{K}^- \mathrm{h}^0}}{\mathrm{B}_{\mathrm{K}^- \mathrm{h}^0} + \mathrm{B}_{\mathrm{K}^- \geq 2\mathrm{h}^0}} \\
G_j^{\mathrm{K}^- \geq 2\mathrm{h}^0} \;&=\; \mathcal{S}_j^{\pi^- \pi^0 \pi^0} (1-f) \frac{\mathrm{B}_{\mathrm{K}^- \geq 2\mathrm{h}^0}}{\mathrm{B}_{\mathrm{K}^- \mathrm{h}^0} + \mathrm{B}_{\mathrm{K}^- \geq 2\mathrm{h}^0}} \\
H_k^{\mathrm{K}^-} \;&=\; \mathcal{T}_k^{\pi^-} f \\
H_k^{\mathrm{K}^- \mathrm{h}^0} \;&=\; \mathcal{T}_k^{\pi^- \pi^0} (1-f) \frac{\mathrm{B}_{\mathrm{K}^- \mathrm{h}^0}}{\mathrm{B}_{\mathrm{K}^- \mathrm{h}^0} + \mathrm{B}_{\mathrm{K}^- \geq 2\mathrm{h}^0}} \\
H_k^{\mathrm{K}^- \geq 2\mathrm{h}^0} \;&=\; \mathcal{T}_k^{\pi^- \pi^0 \pi^0} (1-f) \frac{\mathrm{B}_{\mathrm{K}^- \geq 2\mathrm{h}^0}}{\mathrm{B}_{\mathrm{K}^- \mathrm{h}^0} + \mathrm{B}_{\mathrm{K}^- \geq 2\mathrm{h}^0}} ,
\end{aligned}
$$

and

f is the ratio of the OPAL $\tau^- \to \nu_\tau \, \mathrm{K}^-$ branching ratio to the OPAL $\tau^- \to \nu_\tau \, \mathrm{K}^- \geq 0\mathrm{h}^0$ inclusive branching ratio, and is allowed to float in the fit.

$N^{\mathrm{K}}_{\mathrm{TOTAL}}$ is the total number of charged kaons in the one-prong tau decay sample, as determined in Section 5, and shown in Table 1.

ϵ_l is the efficiency for events from tau decay l in the tau-pair candidate sample to contribute to the one-prong tau decay sample. The $\epsilon_{\mathrm{K}^-\mathrm{h}^0}$, $\epsilon_{\mathrm{K}^-\geq 2\mathrm{h}^0}$, and $\epsilon_{\mathrm{K}^-\geq 1\mathrm{h}^0}$ efficiencies are calculated from the average of the relevant efficiencies appearing in Table 2, weighted by the associated world average branching ratios. All efficiencies have been corrected for biases introduced by the tau-pair selection procedure.

$\mathrm{B}_{\mathrm{K}^-\mathrm{h}^0}$ and $\mathrm{B}_{\mathrm{K}^-\geq 2\mathrm{h}^0}$ are the world average branching ratios for $\tau^-\to\nu_\tau\,\mathrm{K}^-\mathrm{h}^0$ and $\tau^-\to\nu_\tau\,\mathrm{K}^-\geq 2\mathrm{h}^0$ decays, respectively, derived from results presented in reference [17].

S^l_{ij} is the probability, calculated using Monte Carlo generated events, for tau decays of type l in the one-prong tau sample to contribute to the $(i,j)^{\mathrm{th}}$ bin of the $(p, E/p)$ distribution.

$\mathcal{S}^{\pi^-}_j$, $\mathcal{S}^{\pi^-\pi^0}_j$, and $\mathcal{S}^{\pi^-\pi^0\pi^0}_j$ are the corrections to the jth bin of the Monte Carlo E/p distribution of the various one-prong tau decays to pions, as determined from the χ^2 fit using Equation 5.

s^l_i is a normalisation factor used to ensure that the correction to E/p does not affect the shape of the momentum distribution of decays of type l.

T^l_k is the probability, calculated using Monte Carlo generated events, for tau decays of type l in the one-prong tau sample to contribute to the kth bin of the N_{clus} distribution.

$\mathcal{T}^{\pi^-}_j$, $\mathcal{T}^{\pi^-\pi^0}_j$, and $\mathcal{T}^{\pi^-\pi^0\pi^0}_j$ are the corrections to the kth bin of the Monte Carlo N_{clus} distribution of the various one-prong tau decays to pions, as determined in the previous section.

The value of f derived from the result of the fit using Equation 6 is $f = 0.436 \pm 0.013$, where the uncertainty is statistical only. The $\tau^-\to\nu_\tau\,\mathrm{K}^-$ branching ratio derived from this result is:

$$\mathrm{B}_{\mathrm{K}^-} = \mathrm{Br}(\tau^-\to\nu_\tau\,\mathrm{K}^-) = 0.658 \pm 0.024 \pm 0.029\%,$$

where the first uncertainty is statistical and the second is systematic, and the exclusive branching ratio is 60% correlated with the OPAL inclusive $\tau^-\to\nu_\tau\,\mathrm{K}^-\geq 0\mathrm{h}^0$ branching ratio. A summary of the systematic uncertainties on $\mathrm{B}_{\mathrm{K}^-}$ is shown in Table 3.

The statistical uncertainty in $\mathrm{B}_{\mathrm{K}^-}$ due to the statistical uncertainty in the number of kaons within each bin of the $(p, E/p)$ and N_{clus} distributions is assessed by repeating

the fit many times, each time varying the central value of the number of kaons within a particular bin, a bin at a time, by plus, then minus, one statistical standard deviation. The square root of half of the quadrature sum of the net variations produced in the branching ratio is taken as the statistical uncertainty.

The total χ^2 per degree of freedom of the fit using Equation 6 is 63.0/50, where 56.6/46 results from the χ^2 per degree of freedom between the data and predicted $(p, E/p)$ distributions. Figure 5 shows the E/p and N_{clus} distributions of one-prong tau decays with a charged kaon, where the normalisation of the contributions to the predicted distribution comes from the OPAL $\tau^- \to \nu_\tau \, \mathrm{K}^-$ and $\tau^- \to \nu_\tau \, \mathrm{K}^- \geq 0 \mathrm{h}^0$ branching ratios. If the E/p and N_{clus} corrections are not applied, the total χ^2 per degree of freedom from the fit is 79.9/50.

To check for undue variation that may be produced by the choice of binning used in the fit, the above procedure is repeated using various binning schemes. The RMS variation of the results returned by the different fits is less than the statistical uncertainty from the original fit. In addition, a test of the entire fitting procedure (including the calorimeter variable correction procedure described in Sections 6.1 and 6.2) is performed with Monte Carlo generated samples, and verifies that the resulting estimates of f are efficient and unbiased.

6.3   dE/dx Systematic Error

The uncertainty in the N^{K} within each N_{clus} or $(p, E/p)$ bin due to uncertainty in the dE/dx correction factors is determined as in Section 5.2. The dE/dx uncertainties are highly correlated between the bins. Thus the uncertainty in $\mathrm{B}_{\mathrm{K}^-}$ due to the dE/dx systematic uncertainty in the number of kaons within each bin of the $(p, E/p)$ and N_{clus} distributions is assessed by repeating the fit many times, each time varying the the central value of the number of kaons within a particular bin, a bin at a time, by plus, then minus, one standard deviation of the dE/dx systematic uncertainty. Half of the linear sum of the absolute variations produced in the branching ratio is taken as the dE/dx systematic uncertainty in $\mathrm{B}_{\mathrm{K}^-}$, and is shown in Table 3.

6.4   Systematic Uncertainty Associated with the Efficiency Estimation

The uncertainty in the $\tau^- \to \nu_\tau \, \mathrm{K}^-$ branching ratio due to the limited Monte Carlo statistics used to determine the ϵ_{K^-}, $\epsilon_{\mathrm{K}^-\mathrm{h}^0}$, and $\epsilon_{\mathrm{K}^- \geq 2\mathrm{h}^0}$ efficiencies is assessed via the

prior-belief method by modifying Equation 6 such that:

$$\chi^{2\prime} = \chi^2 + \left(\frac{\epsilon'_k - \epsilon_k}{\Delta \epsilon'_k} \right)^2,$$

where

ϵ'_k and $\Delta \epsilon'_k$ are the efficiency and associated uncertainty, due to limited Monte Carlo statistics, for kaons from signal channel k in the tau-pair candidate sample to enter the data sample.

ϵ_k is the efficiency used in the fit for kaons from signal channel k to contribute to the data sample.

In the first iteration of the fit the ϵ_k are allowed to float. In the second, they are fixed to the values from the first iteration. The square root of the quadrature difference in the errors in the branching ratio is taken as the systematic uncertainty associated with the limited Monte Carlo statistics used in the assessment of the efficiencies, and is shown in Table 3.

Various world average exclusive branching ratios are used in the calculation of $\epsilon_{K^-h^0}$ and $\epsilon_{K^- \geq 2h^0}$ (for instance, $\epsilon_{K^-h^0}$ is the average of $\epsilon_{K^-\pi^0}$ and $\epsilon_{K^-K^0}$, weighted by the world average branching ratios $B_{K^-\pi^0}$ and $B_{K^-K^0}$). In addition, these same branching ratios are used to assess the inclusive $\tau^- \to \nu_\tau K^- h^0$ and $\tau^- \to \nu_\tau K^- \geq 2h^0$ branching ratios appearing in Equation 6. The uncertainty in the $\tau^- \to \nu_\tau K^-$ branching ratio due to the uncertainties in these world average branching ratios is assessed by varying the branching ratios, one at a time, by plus, then minus, one standard deviation. The square root of half of the quadrature sum of the net variations produced in the branching ratio is taken as the systematic uncertainty, and is shown in Table 3.

The systematic uncertainty in the efficiency and branching fraction due to the uncertainty associated with the Monte Carlo modelling of the probability for photons to convert to an e^+e^- pair in the OPAL detector material is assessed as described in Section 5.3.

6.5 Systematic Uncertainty Associated with the Modelling of E/p and N_{clus}

The uncertainty in the $\tau^- \to \nu_\tau K^-$ branching ratio due to the statistical uncertainties in the E/p correction factors is assessed using the prior-belief method by modifying Equation 6 such that:

$$\chi^{2\prime} = \chi^2 + (\mathbf{n'} - \mathbf{n})^{\mathbf{T}} \mathbf{V}^{-1} (\mathbf{n'} - \mathbf{n}),$$

where

n′ is a vector containing the central values of the E/p corrections, as obtained from the fit to the $\tau^- \to \nu_\tau \pi^- \leq 2\pi^0$ sample.

n is a vector containing the values of the E/p corrections used in the χ^2 fit.

V is the covariance matrix for the $\mathcal{S}$ correction factors, as obtained from the fit to the $\tau^- \to \nu_\tau \pi^- \leq 2\pi^0$ $(p, E/p)$ and N_{clus} distributions.

In the first iteration, all bins of the three sets of $\mathcal{S}$ corrections are allowed to vary in the fit, and the returned values are found to be consistent with the input values. In the second iteration, the fit is repeated, this time keeping the E/p corrections fixed to the values from the first iteration. The systematic uncertainty in B_{K^-} due to the modelling of E/p is then obtained from the square root of the quadrature difference of the fit uncertainties from the two iterations.

The uncertainty in the $\tau^- \to \nu_\tau K^-$ branching ratio due to the statistical uncertainties in the N_{clus} correction factors is assessed in an analogous fashion. The combined systematic uncertainty in B_{K^-} due to the corrections to the modelling of E/p and N_{clus} is shown in Table 3.

7   Summary and Discussion

From an analysis of the ionisation energy loss of charged particles selected from a sample of 220652 tau decay candidates recorded in the barrel region of the OPAL detector at e^+e^- centre-of-mass energies close to the Z^0 resonance, we determine the branching ratios:

$$\mathrm{Br}(\tau^- \to \nu_\tau K^- \geq 0h^0) = 1.528 \pm 0.039 \pm 0.040\%$$

$$\mathrm{Br}(\tau^- \to \nu_\tau K^-) = 0.658 \pm 0.024 \pm 0.029\%$$

$$\mathrm{Br}(\tau^- \to \nu_\tau K^- \geq 1h^0) = 0.869 \pm 0.031 \pm 0.034\%$$

where the first uncertainties are statistical and the second are systematic. The $\tau^- \to \nu_\tau K^-$ and $\tau^- \to \nu_\tau K^- \geq 1h^0$ branching ratios are 60% and 80% correlated to the $\tau^- \to \nu_\tau K^- \geq 0h^0$ branching ratio, respectively.

Both the inclusive and exclusive branching ratios are in agreement with previous measurements, shown in Table 5, and both contribute significantly to the reduction of the uncertainty on the world averages of the respective quantities.

The theoretical prediction for the $\tau^- \to \nu_\tau\, K^-$ branching ratio is calculated via [20]:

$$
\begin{aligned}
\mathrm{Br}(\tau^- \to \nu_\tau\, K^-) &= \frac{G_F^2 m_\tau^3 \tau_\tau}{16\hbar\pi} f_K^2 |V_{us}|^2 \left(1 - m_K^2/m_\tau^2\right)^2 \\
&= 0.705 \pm 0.008\%,
\end{aligned}
\tag{7}
$$

where the values of $f_K = 0.1598 \pm 0.0015$ GeV and $|V_{us}| = 0.2196 \pm 0.0023$ are both taken from reference [17]. The OPAL measurement is in agreement with this prediction to within 1.3 standard deviations of the combined uncertainties.

The OPAL measurement of the $\tau^- \to \nu_\tau\, K^-$ branching fraction may be used to determine either f_K or $|V_{us}|$ through Equation 7. Assuming $f_K = 0.1598 \pm 0.0015$ GeV, a value of $|V_{us}| = 0.2121 \pm 0.0063$ is obtained. Assuming a value of $|V_{us}| = 0.2196 \pm 0.0023$, a value of $f_K = 0.1544 \pm 0.0046$ GeV is obtained. In both cases, the uncertainty on the determined quantity is dominated by the uncertainty on the $\tau^- \to \nu_\tau\, K^-$ branching fraction.

The theoretical prediction for the $\tau^- \to \nu_\tau\, K^- \geq 0h^0$ branching ratio is obtained by summing the theoretical predictions for the five states appearing in Table 4:

$$
\mathrm{Br}(\tau^- \to \nu_\tau\, K^- \geq 0h^0) = 1.571 \pm 0.043\%.
$$

The OPAL measurement is in agreement with this prediction to within 0.7 standard deviation of the combined uncertainties.

The OPAL collaboration has previously presented results for the tau branching fractions to the $\nu_\tau K^- \pi^- \pi^+ \geq 0\pi^0$, $\nu_\tau \pi^- K^0$, and $\nu_\tau \pi^- K^0 \geq 1\pi^0$ final states [26, 27]. These branching ratios can be combined with the OPAL measurement of the $\tau^- \to \nu_\tau\, K^-$ branching ratio, using isospin relations appearing in [28], to yield an estimate of the branching fraction of the τ^- to final states with strangeness -1:

$$
\mathrm{Br}(\tau^- \to [\text{strangeness}=-1]) = 2.81 \pm 0.16 \pm 0.10\%,
$$

where the calculation of the uncertainties takes into account all correlations between the various OPAL results. The calculation neglects contributions from $\tau^- \to \nu_\tau\, K^- \eta$ to the final state, and assumes that the the $\tau^- \to \nu_\tau\, K^- \pi^- \pi^+ \geq 0\pi^0$ final state is dominated by $\tau^- \to \nu_\tau\, K^- \pi^- \pi^+$, and that the $\tau^- \to \nu_\tau \pi^- K^0 \geq 1\pi^0$ final state is dominated by $\tau^- \to \nu_\tau \pi^- K^0 \pi^0$. The OPAL result is in agreement with the previously published result [29], $\mathrm{Br}(\tau^- \to [\text{strangeness}=-1]) = 2.87 \pm 0.12\%$, to within 0.3σ of the combined uncertainties.

Acknowledgements

References

[1] S. Towers, *Charged Higgs Mass Limits from the $\tau^-\to\nu_\tau\,K^-$ and $K^-\to\bar\nu_l\,l^-(\gamma)$ Branching Fractions*, hep-ex/0004022 (2000).

[2] OPAL Collaboration, K. Ahmet *et al.*, Nucl. Instr. and Meth. **A305** (1991) 275.

[3] M. Hauschild *et al.*, Nucl. Instr. and Meth. **A314** (1992) 74.

[4] H.A. Bethe, Handbuch der Physik 24/1, J.Springer Verlag, Berlin (1933) 491.

[5] E. Fermi, Phys. Rev. Lett. **57** (1940) 485.

[6] R.M. Sternheimer and R.F. Peierls, Phys. Rev. **B3** (1971) 3681.

[7] S. Jadach, B.F.L. Ward, and Z. Wąs, Comp. Phys. Comm. **79** (1994) 503.

[8] S. Jadach, Z. Wąs, R. Decker, and J.H. Kühn, Comp. Phys. Comm. **76** (1993) 361.

[9] *Review of Particle Properties*, Phys. Rev. **D50** (1994) 1173.

[10] T. Sjöstrand, Comp. Phys. Comm. **82** (1994) 74.

[11] F.A. Berends, R. Kleiss, and W. Hollik, Nucl. Phys. **B304** (1988) 712.

[12] S. Jadach, W. Placzek, and B.F.L. Ward, Phys. Lett. **B390** (1997) 298.

[13] R. Bhattacharya, J. Smith, and G. Grammer, Phys. Rev. **D15** (1977) 3267;
J. Smith, J.A.M. Vermaseren, and G. Grammer, Phys. Rev. **D15** (1977) 3280.

[14] J. Hilgart, R. Kleiss, and F. Le Diberder, Comp. Phys. Comm. **75** (1993) 191.

[15] J. Allison *et al.*, Nucl. Instr. and Meth. **A317** (1992) 47.

[16] OPAL Collaboration, K. Ackerstaff *et al.*, Eur. Phys. J. **C4** (1998) 193.

[17] *Review of Particle Physics*, Eur. Phys. J. C, **Vol. 3**, Number 1-4 (1998).

[18] OPAL Collaboration, G. Alexander *et al.*, Phys. Lett. **B388** (1996) 437.

[19] ALEPH Collaboration, R. Barate *et al.*, Eur. Phys. J. **C10** (1999) 1.

[20] B.C. Barish and R. Stroynowski, Phys. Rep. **157** (1988) 1.

[21] S. Eidelman *et al.*, Nucl. Phys. B (Proc. Suppl.), **55C** (1997) 181.

[22] E. Mirkes, Nuclear Physics B (Proc. Suppl.), **55C** (1997) 169.

[23] DELPHI Collaboration, P. Abreu *et al.*, Phys. Lett. **B334** (1994) 435.

[24] CLEO Collaboration, M. Battle *et al.*, Phys. Rev. Lett. **73** (1994) 1079.

[25] DELCO Collaboration, G.B. Mills *et al.*, Phys. Rev. Lett. **52** (1984) 1944.

[26] OPAL Collaboration, G. Abbiendi *et al.*, Eur. Phys. J. **C13** (2000) 197.

[27] OPAL Collaboration, G. Abbiendi *et al.*, Eur. Phys. J. **C13** (2000) 213.

[28] A. Rouge, Z. Phys. **C70** (1996) 65.

[29] ALEPH Collaboration, R. Barate *et al.*, Eur. Phys. J. **C11** (1999) 599.

N_τ	220652
$f^{\mathrm{non}-\tau}$	$1.56 \pm 0.10\%$
# in one-prong sample	143528
N^π_{TOTAL}	$75566 \pm 389 \pm 246$
N^π_{bkgnd}	89 ± 16
$\epsilon_{\pi^- \geq 0h^0}$	$0.720 \pm 0.001 \pm 0.001$
$N^{\mathrm{K}}_{\mathrm{TOTAL}}$	$2526 \pm 64 \pm 52$
$N^{\mathrm{K}}_{\mathrm{bkgnd}}$	9 ± 4
$\epsilon_{\mathrm{K}^- \geq 0h^0}$	$0.759 \pm 0.006 \pm 0.007$

Table 1: Pion and kaon composition of the one-prong tau decay candidate sample, as estimated by the likelihood fit to the measured dE/dx of tracks in the sample. The first uncertainty on N^π_{TOTAL} and $N^{\mathrm{K}}_{\mathrm{TOTAL}}$ is the statistical uncertainty from the fit, and the second is due to the systematic uncertainty in the dE/dx correction factors. Also shown are the estimated backgrounds in N^π_{TOTAL} and $N^{\mathrm{K}}_{\mathrm{TOTAL}}$, along with the efficiencies for signal events to contribute to the one-prong tau decay sample. The first uncertainty on each efficiency estimate is due to the limited statistics of the Monte Carlo generated samples, while the second is due to the uncertainty in the various branching ratios used to calculate the efficiency, as listed in Table 2.

τ^- Decay Mode	BR (%)	Efficiency
$\tau^- \rightarrow \nu_\tau \, \pi^-$	11.08 ± 0.13	0.810 ± 0.003
$\tau^- \rightarrow \nu_\tau \, \pi^- \pi^0$	25.32 ± 0.15	0.725 ± 0.002
$\tau^- \rightarrow \nu_\tau \, \pi^- \mathrm{K}^0$	0.83 ± 0.08	0.604 ± 0.007
$\tau^- \rightarrow \nu_\tau \, \pi^- \pi^0 \pi^0$	9.15 ± 0.15	0.642 ± 0.003
$\tau^- \rightarrow \nu_\tau \, \pi^- \mathrm{K}^0 \mathrm{K}^0$	0.121 ± 0.021	0.454 ± 0.016
$\tau^- \rightarrow \nu_\tau \, \pi^- \mathrm{K}^0 \pi^0$	0.39 ± 0.05	0.550 ± 0.015
$\tau^- \rightarrow \nu_\tau \, \pi^- \pi^0 \pi^0 \pi^0$	1.11 ± 0.14	0.569 ± 0.005
$\tau^- \rightarrow \nu_\tau \, \pi^- \eta + \geq 0\pi^0$	0.188 ± 0.025	0.655 ± 0.024
$\tau^- \rightarrow \nu_\tau \, \mathrm{K}^-$	-	0.843 ± 0.010
$\tau^- \rightarrow \nu_\tau \, \mathrm{K}^- \pi^0$	0.52 ± 0.05	0.757 ± 0.011
$\tau^- \rightarrow \nu_\tau \, \mathrm{K}^- \mathrm{K}^0$	0.159 ± 0.024	0.661 ± 0.013
$\tau^- \rightarrow \nu_\tau \, \mathrm{K}^- \eta$	0.027 ± 0.006	0.757 ± 0.011
$\tau^- \rightarrow \nu_\tau \, \mathrm{K}^- \pi^0 \pi^0$	0.080 ± 0.027	0.664 ± 0.025
$\tau^- \rightarrow \nu_\tau \, \mathrm{K}^- \mathrm{K}^0 \pi^0$	0.151 ± 0.029	0.544 ± 0.012
$\tau^- \rightarrow \nu_\tau \, \mathrm{K}^- \pi^0 \pi^0 \pi^0$	0.035 ± 0.024	0.643 ± 0.025
$\tau^- \rightarrow \nu_\tau \, \mathrm{K}^- \mathrm{K}^0 \pi^0 \pi^0$	0.000 ± 0.018	0.560 ± 0.012

Table 2: Branching ratios and efficiencies used to estimate the efficiencies for the $\tau^- \rightarrow \nu_\tau \, \mathrm{K}^- \geq 0h^0$ and $\tau^- \rightarrow \nu_\tau \, \pi^- \geq 0h^0$ decays in the tau-pair sample to contribute to the one-prong sample. The $\tau^- \rightarrow \nu_\tau \, \mathrm{K}^- \mathrm{K}^0 \pi^0 \pi^0$ branching fraction is estimated from the result appearing in [19].

	Branching Ratios (%)		
	$B_{\pi^- \geq 0h^0}$	$B_{K^- \geq 0h^0}$	B_{K^-}
Central value	48.17	1.528	0.658
σ (stat)	± 0.25	± 0.039	± 0.024
σ (dE/dx sys)	± 0.16	± 0.032	± 0.017
σ (E/p and N_{clus} modelling)	-	-	± 0.014
σ (photon conversion modelling)	± 0.68	± 0.015	± 0.003
σ (MC stat)	± 0.09	± 0.012	± 0.006
σ (efficiency sys)	± 0.05	± 0.014	± 0.017

Table 3: Summary of the branching ratio central values and sources of uncertainties. The second-to-last uncertainty is the systematic uncertainty arising from the limited statistics of the Monte Carlo generated samples used to estimate the selection efficiencies. The last uncertainty is due to the systematic uncertainty in the efficiency correction arising from the uncertainties in the various world average branching ratios used in the weighted average calculation of the $\tau^- \to \nu_\tau K^- \geq 0h^0$, $\tau^- \to \nu_\tau \pi^- \geq 0h^0$, and $\tau^- \to \nu_\tau K^- \geq 1h^0$ efficiencies.

τ^- DECAY MODE	THEORY BR (%)	
$\tau^- \to \nu_\tau K^-$	0.705 ± 0.008	[20]
$\tau^- \to \nu_\tau K^- \pi^0$	0.48 ± 0.02	[20]
$\tau^- \to \nu_\tau K^- K^0$	0.111 ± 0.031	[21]
$\tau^- \to \nu_\tau K^- \pi^0 \pi^0$	0.12 ± 0.02	[22]
$\tau^- \to \nu_\tau K^- K^0 \pi^0$	0.155 ± 0.005	[22]

Table 4: Theoretical predictions for tau branching ratios to the dominant one-prong final states that include a charged kaon.

τ^- DECAY MODE	EXPERIMENT BR (%)	
$\tau^-\!\to\!\nu_\tau\,\mathrm{K}^-$	$0.696 \pm 0.025 \pm 0.014$	ALEPH99[19]
	0.85 ± 0.18	DELPHI94[23]
	$0.66 \pm 0.07 \pm 0.09$	CLEO94[24]
	0.59 ± 0.18	DELCO84[25]
	$0.658 \pm 0.024 \pm 0.029$	(this analysis)
$\tau^-\!\to\!\nu_\tau\,\mathrm{K}^- \geq 0\mathrm{h}^0$	$1.52 \pm 0.04 \pm 0.04$	ALEPH99[19]
	1.54 ± 0.24	DELPHI94[23]
	$1.60 \pm 0.12 \pm 0.19$	CLEO94[24]
	1.71 ± 0.29	DELCO84[25]
	$1.528 \pm 0.039 \pm 0.040$	(this analysis)

Table 5: Summary of the $\tau^-\!\to\!\nu_\tau\,\mathrm{K}^-$ and $\tau^-\!\to\!\nu_\tau\,\mathrm{K}^- \geq 0\mathrm{h}^0$ branching ratios.
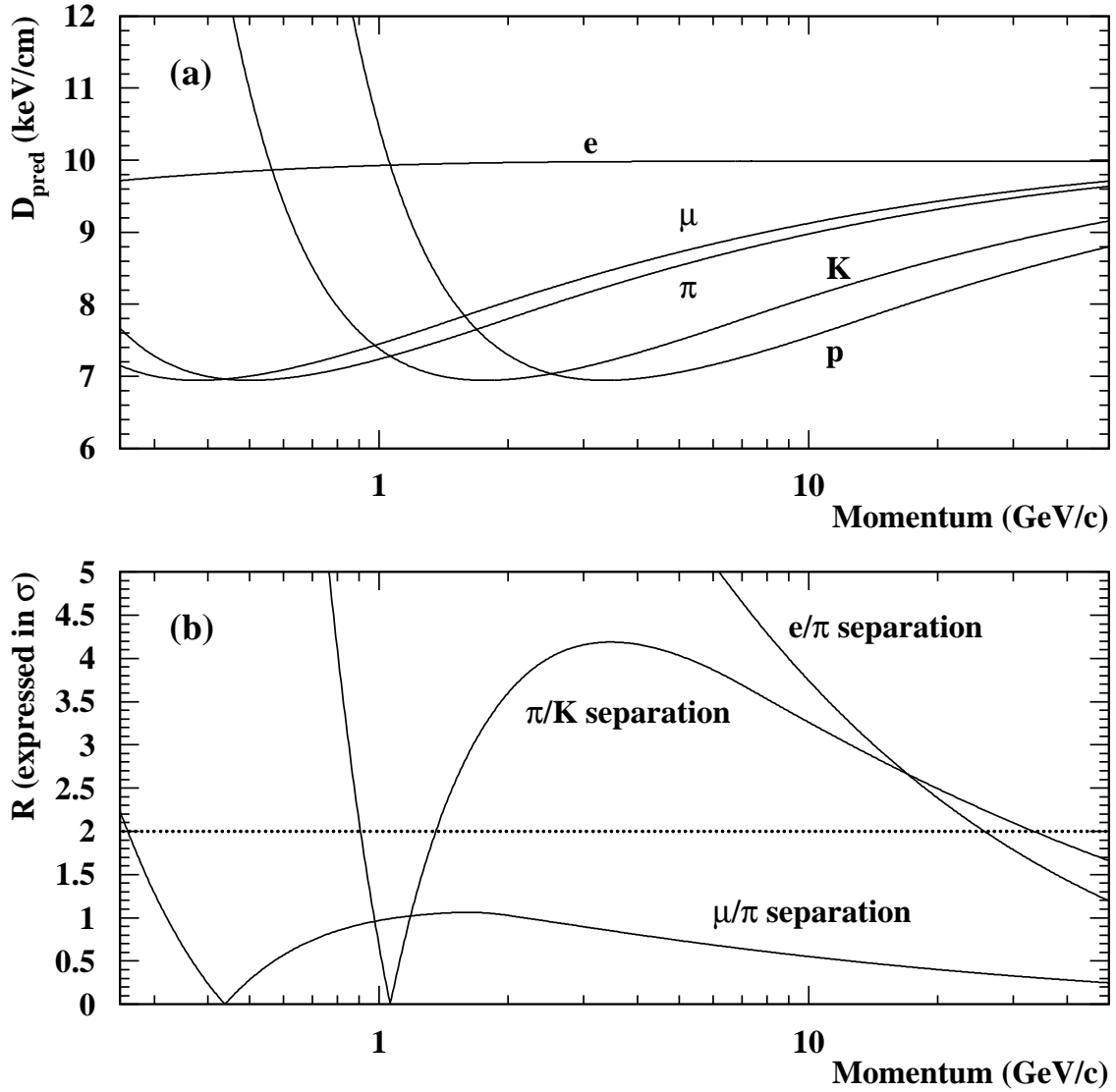
Figure 1: (a) shows the ionisation energy loss D_{pred} as a function of the momentum for various particles in the OPAL jet chamber. (b) shows the resolution power $\mathcal{R}_{ij}$ expressed in terms of the $\mathrm{d}E/\mathrm{d}x$ resolution σ, for various pairs of particle species i and j.
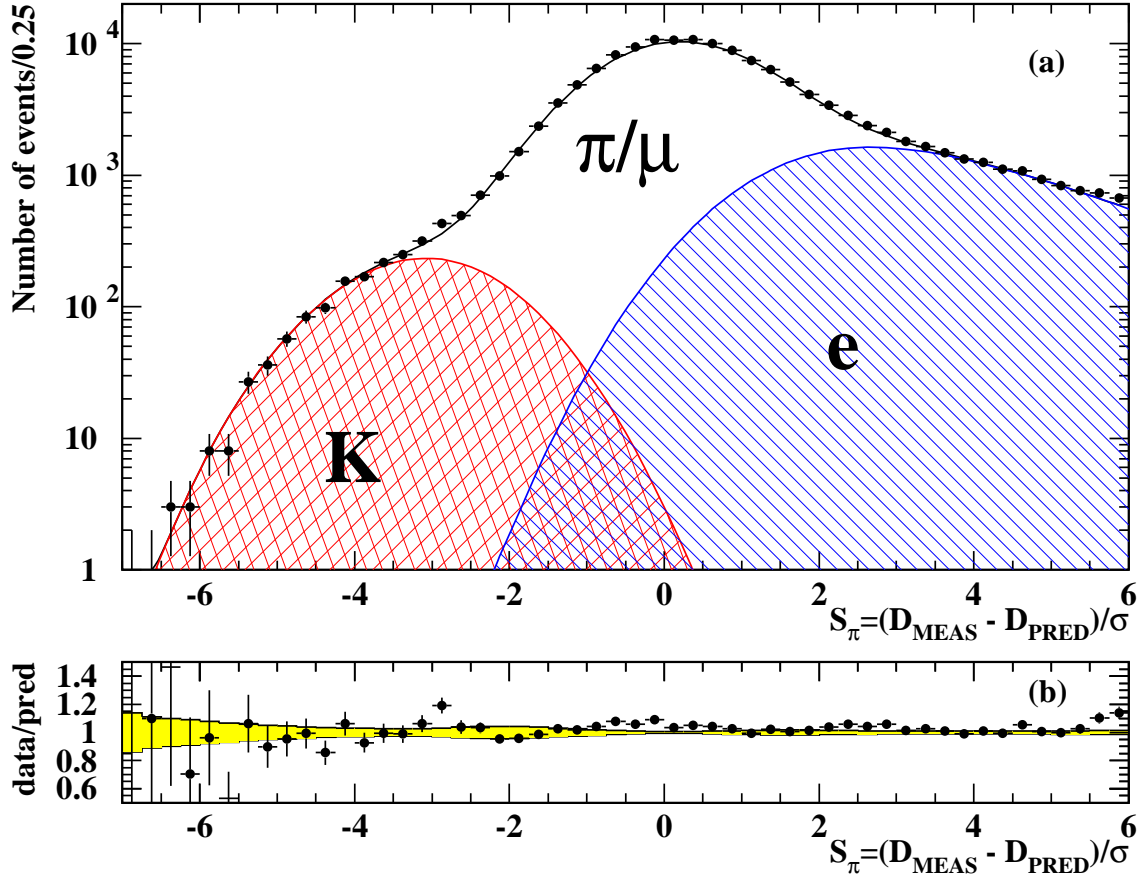
Figure 2: (a) is the stretch dE/dx distribution under a pion hypothesis for tracks in the data $\tau^- \to \nu_\tau \, h^- \geq 0h^0$ candidate sample (points). The overlaid curves are the predicted distributions for kaons, pions, muons, and electrons in the sample. The normalisation of the curves is obtained from the results of the likelihood fit described in Section 5. (b) is the distribution of the data points in plot (a) divided by the predicted distribution. The shaded area represents the approximate one sigma dE/dx systematic uncertainty envelope on the predicted distribution. The χ^2 per degree of freedom between the data and a line centred at $y = 1$, taking into account both statistical and dE/dx systematic uncertainties, is 36.5/47.
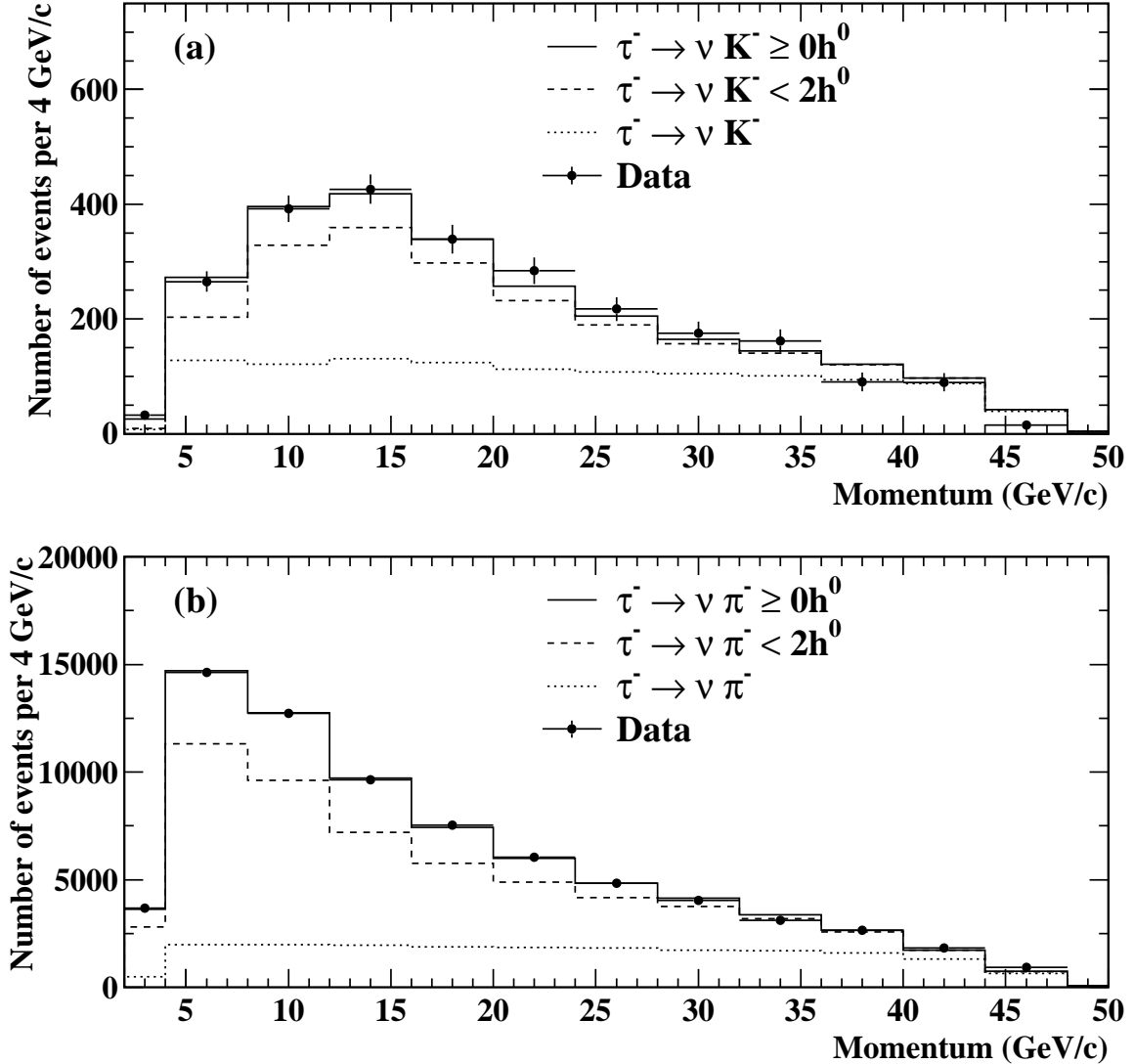
Figure 3: (a) and (b) are the momentum distributions of charged kaons and pions, respectively, in the data one-prong tau decay sample (points), as obtained from the results of the dE/dx likelihood fit described in Section 5. The histograms are the momentum distributions predicted by Monte Carlo generated $\tau^- \to \nu_\tau K^- \geq 0h^0$ and $\tau^- \to \nu_\tau \pi^- \geq 0h^0$ events. The overall normalisation of the predicted distributions comes from the results of the dE/dx likelihood fit, while the relative normalisation of the exclusive decay modes contributing to the sample is taken from the relevant world average branching ratios appearing in reference [17].
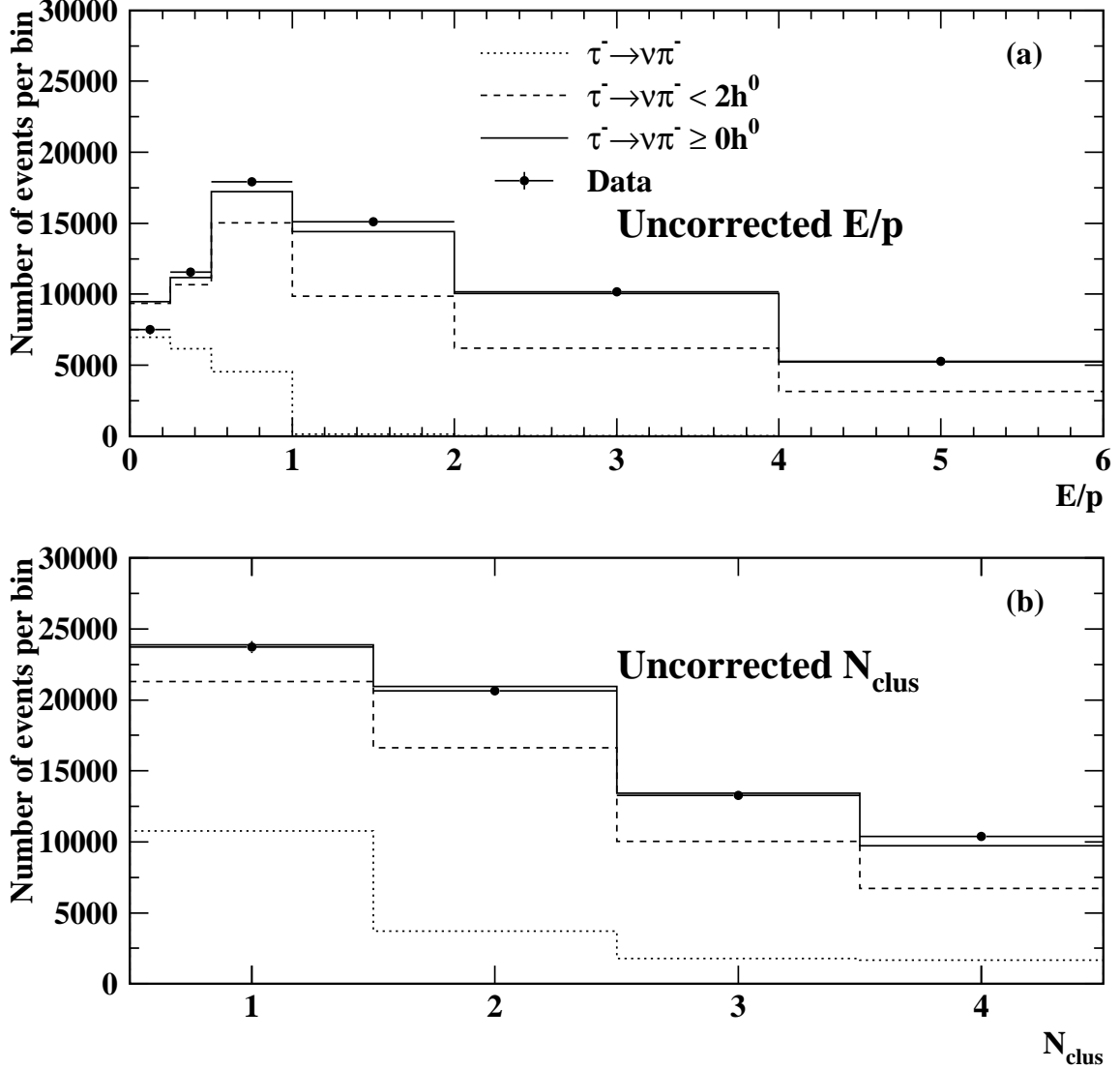
Figure 4: (a) and (b) are the uncorrected E/p and N_{clus} distributions, respectively, of Monte Carlo generated $\tau^- \to \nu_\tau \, \pi^- \geq 0\mathrm{h}^0$ decays (histograms), along with the E/p and N_{clus} distributions of data one-prong tau decays with a charged pion in the final state (points). The relative normalisations of the various exclusive tau decays that contribute to the sample are taken from the relevant world average branching ratios listed in reference [17]. Backgrounds are on the order of 0.2% or less and are neglected in the plots. The last bin in each of the distributions contains overflow events.
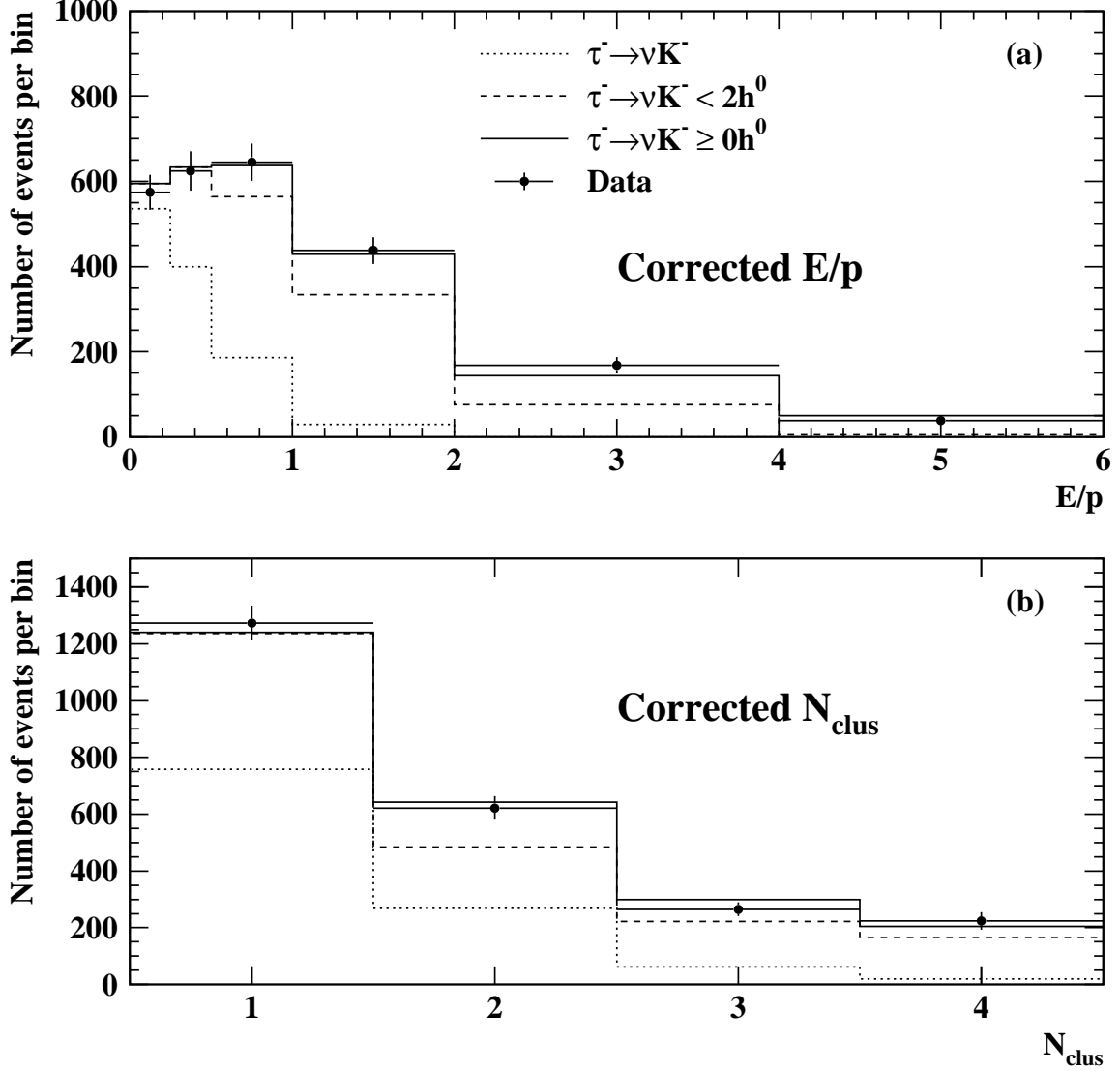
OPAL

Figure 5: (a) and (b) are the corrected E/p and N_{clus} distributions, respectively, of Monte Carlo generated $\tau^- \to \nu_\tau\, K^- \geq 0h^0$ decays (histogram), along with the E/p and N_{clus} distributions of data one-prong tau decays with a charged kaon in the final state (points). The overall normalisation of Monte Carlo distributions is obtained from the results of the dE/dx likelihood fit using Equation 2, while the normalisation of the $\tau^- \to \nu_\tau\, K^-$ component is obtained from the results of the χ^2 fit using Equation 6. Backgrounds are on the order of 0.4% or less and are neglected in this plot. The last bin in each of the distributions contains overflow events.